RISET
Geologi dan Pertambangan
Indonesian Journal of Geology and Mining
https://jrisetgeotam.lipi.go.id
LIPI

Research article

Coseismic and postseismic deformation from the 2007 Bengkulu earthquake based on GPS Data

Riset Geologi dan Pertambangan
Indonesian Journal of Geology and Mining
Vol.31, No 2, pages 98–107

doi:
10.14203/risetgeotam2021.v31.1182

Keywords:
The 2007 Bengkulu earthquake,
GPS data,
coseismic displacements,
postseismic decay,
strain.

Corresponding author:
Irwan Meilano
E-mail address: irwanm@itb.ac.id

Article history
Received: 27 August 2021
Revised: 12 September 2021
Accepted: 28 September 2021

Irwan Meilano[1], Susilo Susilo[2], Endra Gunawan[3], Suchi Rahmadani[4,5]

[1]Faculty of Earth Sciences and Technology, Institute of Technology Bandung (ITB), Bandung, Indonesia
[2]Geospatial Information Agency, Cibinong, Indonesia
[3]Faculty of Mining and Petroleum Engineering, Institute of Technology Bandung (ITB), Bandung, Indonesia
[4]Geodesy and Geomatics Study Program, Institute of Technology Bandung (ITB), Bandung, Indonesia
[5]Center for Earthquake Science and Technology, Institute of Technology Bandung (ITB), Bandung, Indonesia

ABSTRACT On September 12, 2007, an M8.5 megathrust earthquake occurred along the Sunda trench near Bengkulu, West Sumatra. GPS data in Sumatra have indicated the coseismic and postseismic deformations resulting from this earthquake. Our estimate of coseismic displacements suggests that the earthquake displaced up to ~1.8m at GPS stations located north of the epicenter. Moreover, our principal strain estimation in the region suggests that the maximum coseismic extensional strain is ~40 ppm. Our analysis of GPS data in the region suggests that the postseismic decay of the 2007 Bengkulu earthquake was 46 days, estimated using a logarithmic function.

INTRODUCTION

During the earthquake cycle, which is generally divided into deformations in three phases interseismic (Hanifa et al., 2014; Ohkura et al., 2015), coseismic (Ito et al., 2016; Gunawan et al., 2017a), and postseismic (Anugrah et al., 2015; Pratama et al., 2017) surface deformation can be observed using various geodetic tools. Modern equipment, such as the Global Positioning System (GPS; Alif et al., 2016), Interferometric Synthetic Aperture Radar (InSAR; Tung and Masterlark, 2016), and/or levelling (Murase et al., 2016), has been widely used to analyze crustal deformations and tectonic conditions in a region.

Along the subduction zone, deformation might be observed as a result of seismic (Ito et al., 2012) and/or aseismic activity. Aseismic conditions can occur, as in the case of aseismic slip after the 2006 Java tsunami earthquake (Gunawan et al., 2016a) or the cases of slow slip events along Hikurangi subduction zone in New Zealand (Wallace et al., 2016) and Tokai region in Japan (Hirose and Obara, 2006). However, when the fault couples, the energy may be released as a megathrust earthquake (Gusman et al., 2015; Gunawan et al., 2016b; Gunawan et al., 2017b). One example is the September 12, 2007 Bengkulu earthquake, which occurred along the Sunda trench in West Sumatra, Indonesia.

The Sunda trench is considered to be an active region, with several occurrences of magnitude 8 or 9 earthquakes during the last decade, such as the 2004 M9.2 Sumatra-Andaman earthquake (Rhie et al., 2007) and the 2005 M8.6 Nias earthquake (Konca et al., 2007). Previous studies have analyzed the coseismic deformation of the 2007 Bengkulu earthquake using joint GPS data, field measurements of uplift, synthetic aperture radar (SAR) interferometry (InSAR) and seismological records (Konca et al., 2008), tide-gauge data (Lorito et al., 2008), or a combination of InSAR, tide-gauge, and bottom-pressure-sensor data (Gusman et al., 2010). The postseismic deformation as recorded by GPS in Sumatra has also been identified (Feng et al., 2015). Unfortunately, these findings did not clearly identify the mechanisms of postseismic deformation of the 2007 Bengkulu earthquake.

Here, we revisit the coseismic and postseismic deformation of the 2007 Bengkulu earthquake. Our analysis involves newly available, never-before-published GPS data for the region. All available GPS data are then used to investigate the postseismic decay with a numerical equation defined by exponential and logarithmic functions and estimate the earthquake's coseismic displacement. The strain analysis is then used to estimate the affected region based on the coseismic displacement at every GPS station.

GPS Data and Processing

GPS data were obtained from the Sumatran GPS Array (SuGAr; Feng et al., 2015) and the Indonesian Continuously Operating Reference Stations (Ina-CORS; Gunawan et al., 2016c) networks. Figure 1 shows the location of the GPS stations used in this study.

Daily solutions of these GPS data were then processed using GAMIT/GLOBK (Herring et al., 2010a; Herring et al., 2010b). We followed the GPS analysis procedure of Gunawan et al. (2016a). Along with 20 regionalIGS (International GNSS Service) stations, we tied this local network to the ITRF2008 reference frame (Altamimi et al., 2011). We analyzed daily solutions along with atmospherically used, loose-constraint, prior GPS phase observations; the orbit and earth-orientation parameters were fixed.

We then combined these positions and the covariance with global GPS solutions computed as part of MIT's processing for the IGS. During this process, we mapped the loosely constrained solution onto a well-constrained ITRF2008 reference frame (Altamimi et al., 2011) by minimizing the position and velocity differences of selected sites with respect to a priori values defined by the IGb08 realization.

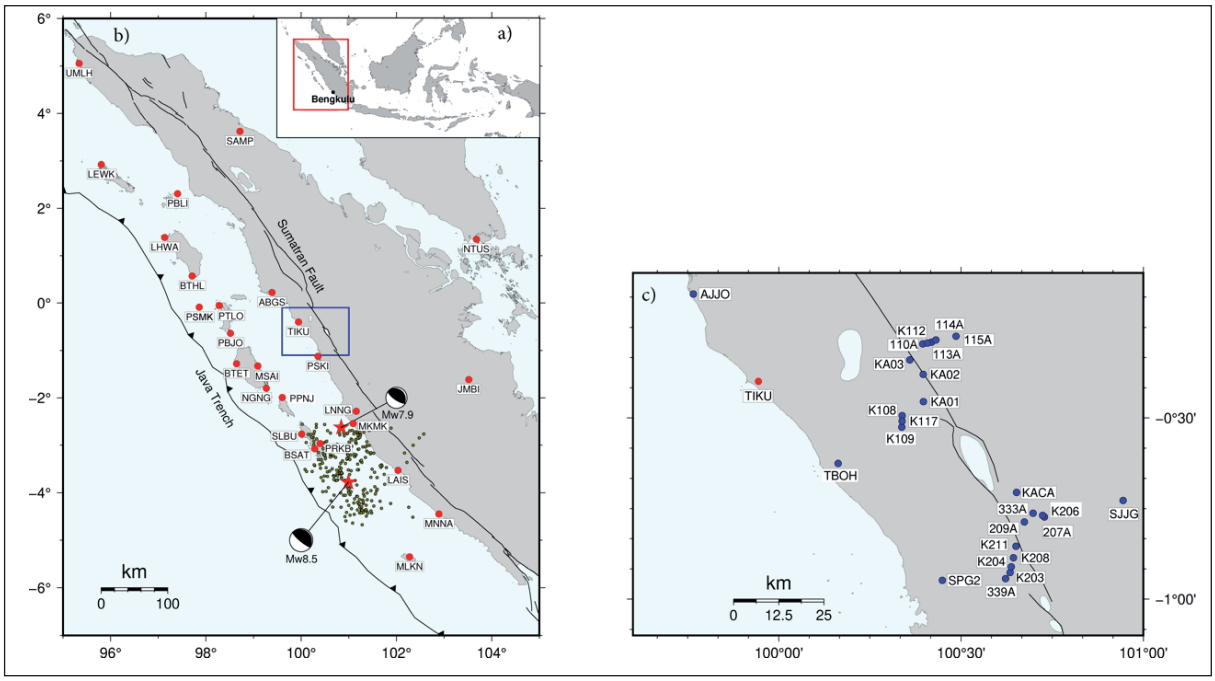

Figure 1. Distribution of GPS stations of this study for (left) regional setting along Sumatra and surrounding region, (right) detail view at western Sumatra. Black lines are delineation of Java trench and Sumatran Fault. Continuous GPS stations show with red dots, while campaign GPS stations show with blue dots. Red stars are the epicenter of the 2007 Mw8.5 Bengkulu earthquake and the 2010 Mw7.9 Mentawai earthquake from Global Centroid-Moment-Tensor catalogue (Ekström et al., 2012), respectively. Dark green dots represent 45 days aftershock after the earthquake.

Postseismic Decay and Coseismic Displacements

Using the estimated daily solutions, we first analyzed the postseismic decay of the 2007 Bengkulu earthquake. Our estimation for fitting the timeseries data was based on the logarithmic function defined in Marone et al. (1991). As a comparison, we also analyzed postseismic decay by fitting the timeseries data using an exponential function, defined as following Savage and Prescott (1978). In these functions, t is the time duration after the earthquake, $u(t)$ is north and east displacements, c is offset, a is amplitude, and τ_{log} and τ_{exp} are postseismic decay time from the logarithmic and exponential functions, respectively.

In our analysis, we searched for τ_{log} between 10 and 100 days and for τ_{exp} between 300 and 500 days. Thus, the values for a and c differ with values of τ_{log} and τ_{exp}. Misfits are calculated using root mean square (RMS), defined as, where and represent the data and model, respectively, while n is the total number of data points. Our calculation shows that the best-fit results for τ_{log} and τ_{exp}, are at 46±1 day and 3811 day (Figure 2). Based on these values, the RMS of logarithmic and exponential functions to the GPS data are 0.84 cm (Table 1) and 0.86 cm (Table 2), respectively.

Second, we analyzed coseismic displacements using tsview (Herring, 2003) applied to both campaign and continuous data. We used the logarithmic function, which had less misfit than the exponential one. The coseismic displacements were then calculated using a projection of logarithmic function on the day after the 2007 Bengkulu earthquake subtracted from the data before the earthquake. Maximum coseismic displacement was ~1.8m at PRKB station, located north of the epicenter. We compare our GPS observation data to modeled displacement calculated on an elastic half-space model (Okada, 1992) using coseismic slip distribution of Konca et al. (2008). In general, our GPS data fits the model very well. Figure 3 shows the observation and modeled coseismic displacements at every GPS station.

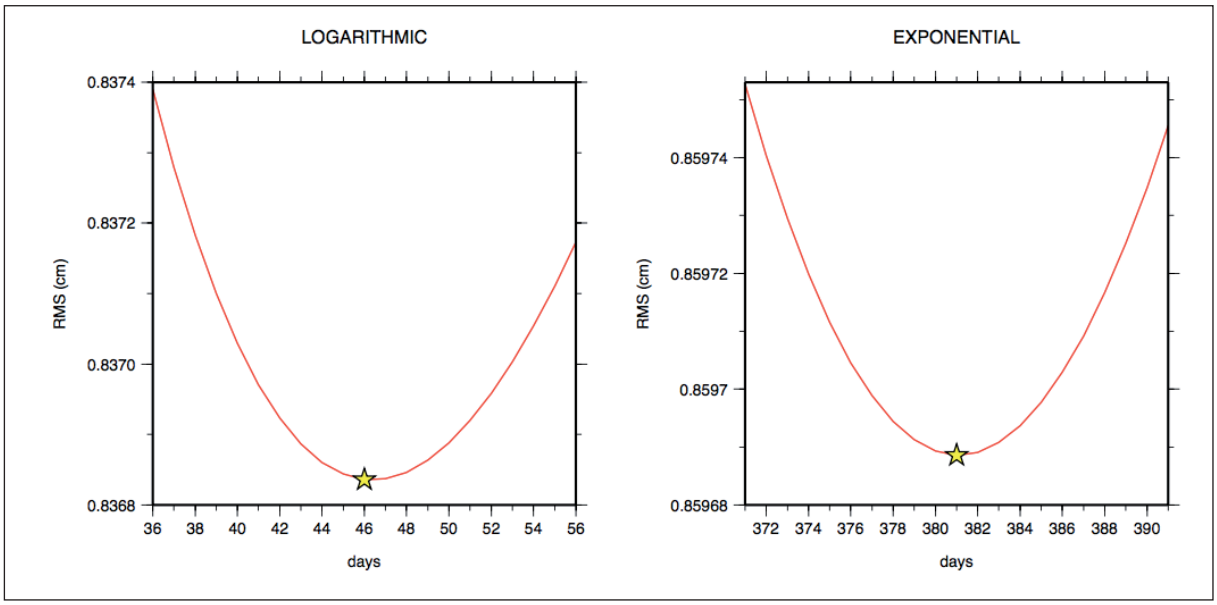

Figure 2. Postseismic decay from (left) logarithmic, and (right) exponential functions. Best-fit is shown by star symbol.

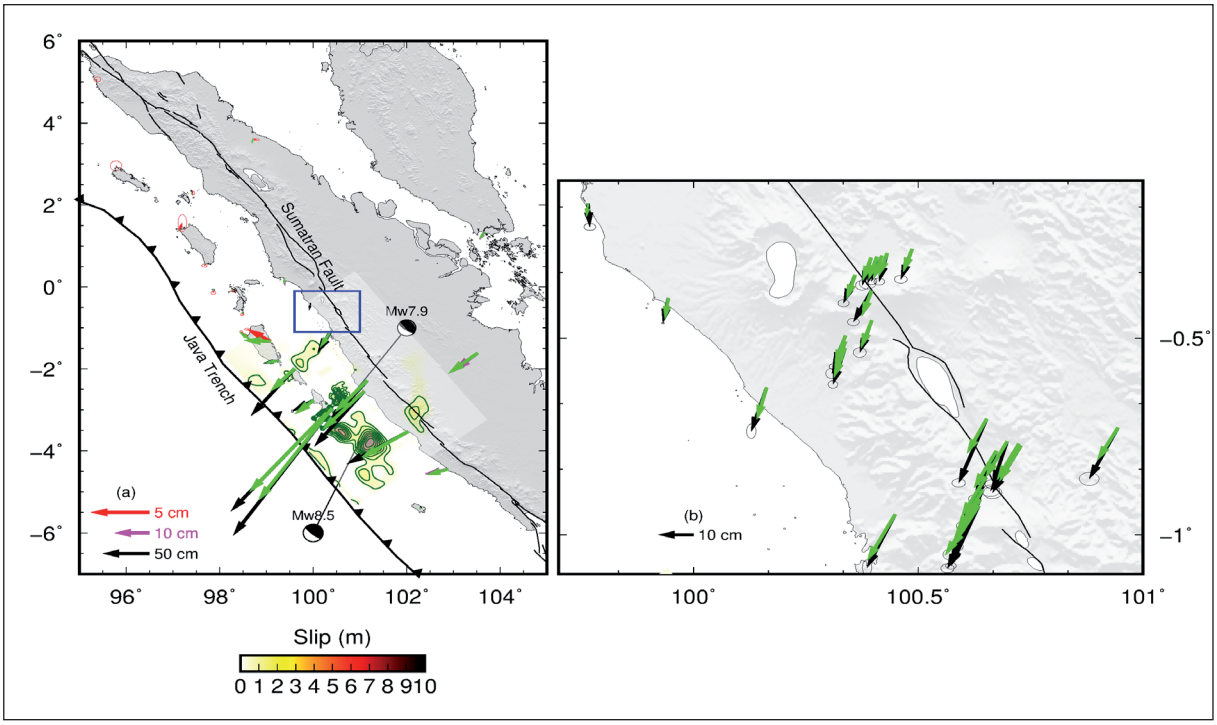

Figure 3. Coseismic displacement at every GPS station. Note the arrow scale is differences. Coseismic slip is based on Konca et al. (2008) and contoured every 0.5 m. Red, magenta, and black arrows are coseismic displacements from GPS with different scales. Green arrows are coseismic displacement from modeling based on slip distribution from Konca et al. (2008), and the scales are similar to the red, magenta, black arrows. The focal mechanisms are from Global Centroid-Moment-Tensor catalogue (Ekström et al., 2012). The right side is the detailed view coseismic displacement from the blue rectangle in the left side. Topography is from Becker et al. (2009).

Table 1. Postseismic parameters calculated using the logarithmic function at τ_{log} 46 days

Type	Stations	c		a		RMS
		N (cm)	E (cm)	N (cm)	E (cm)	
Camp.	110A	0.13±0.31	0.03±0.57	-0.83±0.13	-0.42±0.24	0.39
	113A	0.21±0.44	0.00±0.54	-1.04±0.19	-0.55±0.23	0.42
	114A	0.20±0.53	0.10±0.44	-1.07±0.22	-0.61±0.19	0.42
	115A	0.31±0.54	-0.03±0.65	-1.00±0.22	-0.17±0.26	0.52
	207A	0.27±0.61	0.30±0.16	-1.68±0.26	-0.85±0.07	0.38
	209A	0.26±0.49	0.18±0.38	-1.51±0.21	-1.03±0.16	0.37
	333A	0.20±0.89	0.21±0.80	-1.97±0.36	-1.10±0.33	0.74
	339A	-0.18±0.95	0.64±1.21	-0.85±0.39	-2.01±0.50	0.94
	K108	-0.42±0.99	-0.12±0.81	-0.15±0.41	-0.47±0.33	0.80
	K109	-0.24±0.70	-0.09±0.62	-0.15±0.30	-0.50±0.26	0.57
	K112	0.32±0.40	0.05±0.18	-1.14±0.17	-0.47±0.08	0.27
	K117	-0.30±0.93	0.05±0.62	-0.26±0.40	-0.70±0.26	0.69
	K203	-0.03±0.95	0.63±0.98	-1.06±0.40	-1.66±0.42	0.81
	K204	-0.20±0.85	0.62±0.92	-0.34±0.36	-2.11±0.39	0.75
	K206	0.38±0.49	0.24±0.48	-1.92±0.21	-0.59±0.20	0.41
	K208	-0.03±0.79	0.86±0.86	-0.83±0.34	-1.83±0.37	0.71
	K211	0.04±0.79	0.51±0.47	-1.17±0.34	-1.68±0.20	0.55
	KA01	-0.08±0.43	-0.32±1.53	-0.37±0.18	0.02±0.63	0.99
	KA02	0.01±0.48	-0.67±2.07	-0.69±0.20	0.45±0.89	1.29
	KA03	-0.01±0.50	-0.70±2.25	-0.54±0.21	0.12±0.96	1.41
	KACA	0.10±2.27	-1.88±3.08	0.05±0.83	0.80±1.12	0.60
	SJJG	-0.45±0.72	1.64±3.60	0.20±0.26	-0.76±1.32	0.57
	SPG2	0.14±0.42	0.54±0.63	-0.82±0.17	-1.51±0.25	0.47
	TBOH	0.13±0.22	-0.27±0.62	-0.60±0.12	0.40±0.34	0.90
Cont.	BSAT	-6.64±0.26	-1.97±0.20	-3.37±0.11	-5.56±0.08	2.28
	BTET	-3.92±0.12	-0.41±0.03	4.70±0.05	0.41±0.01	0.83
	LAIS	-2.37±0.06	0.84±0.05	-2.79±0.02	-5.84±0.02	0.55
	LNNG	-4.04±0.11	1.32±0.10	-2.95±0.04	-5.82±0.04	1.01
	MKMK	-3.57±0.08	0.67±0.04	-3.49±0.03	-6.49±0.02	0.58
	MLKN	-2.90±0.09	1.45±0.06	2.31±0.04	-1.27±0.02	0.71
	MNNA	-1.40±0.06	1.67±0.06	1.26±0.02	-2.42±0.02	0.54
	MSAI	-1.51±0.12	1.11±0.16	2.52±0.05	-0.81±0.06	1.08
	NGNG	-10.06±0.34	-5.09±0.22	5.42±0.13	1.03±0.08	1.44
	PBJO	-2.60±0.10	-0.41±0.04	3.10±0.04	0.31±0.02	0.70
	PKRT	-2.15±0.11	5.42±0.08	0.86±0.04	-4.07±0.03	0.52
	PPNJ	-2.21±0.10	-2.41±0.05	-0.43±0.04	-2.12±0.02	0.73
	PRKB	-5.68±0.16	-1.76±0.05	-0.49±0.06	-5.23±0.02	1.04
	PSKI	-2.00±0.10	1.11±0.06	-0.16±0.04	-1.95±0.02	0.70
	SLBU	0.87±0.65	1.05±0.11	-10.95±0.26	-2.42±0.04	4.15
	TIKU	-2.73±0.09	-0.09±0.04	1.70±0.03	-0.21±0.02	0.65
				Average		0.84

Table 2. Postseismic parameter calculated using the exponential function at τexp 381 days

Type	Stations	c		a		RMS
		N (cm)	E (cm)	N (cm)	E (cm)	
Camp.	110A	-0.02+0.25	-0.03+0.40	-2.59+0.48	-1.35+0.76	0.40
	113A	0.00+0.35	-0.10+0.38	-3.25+0.66	-1.72+0.73	0.44
	114A	-0.02+0.41	0.00+0.31	-3.34+0.78	-1.94+0.59	0.44
	115A	0.12+0.33	-0.05+0.39	-3.12+0.70	-0.55+0.82	0.52
	207A	-0.07+0.49	0.14+0.08	-5.23+0.93	-2.69+0.15	0.42
	209A	-0.04+0.38	-0.03+0.31	-4.71+0.73	-3.22+0.59	0.42
	333A	-0.23+0.59	-0.01+0.49	-6.09+1.25	-3.41+1.04	0.78
	339A	-0.39+0.59	0.22+0.75	-2.59+1.25	-6.24+1.58	0.97
	K108	-0.49+0.61	-0.20+0.50	-0.38+1.29	-1.48+1.05	0.81
	K109	-0.30+0.51	-0.19+0.45	-0.41+0.96	-1.55+0.86	0.58
	K112	0.11+0.31	-0.04+0.15	-3.59+0.60	-1.46+0.28	0.30
	K117	-0.39+0.68	-0.06+0.44	-0.75+1.29	-2.24+0.83	0.69
	K203	-0.26+0.68	0.29+0.71	-3.28+1.31	-5.18+1.36	0.84
	K204	-0.28+0.60	0.17+0.70	-1.05+1.15	-6.55+1.34	0.79
	K206	-0.01+0.41	0.12+0.34	-6.00+0.78	-1.85+0.66	0.45
	K208	-0.20+0.57	0.54+0.58	-2.59+1.09	-5.78+1.11	0.70
	K211	-0.21+0.58	0.18+0.37	-3.63+1.11	-5.27+0.71	0.59
	KA01	-0.18+0.28	-0.28+0.95	-1.11+0.58	0.01+1.98	0.99
	KA02	-0.14+0.37	-0.59+1.48	-2.14+0.69	1.43+2.80	1.30
	KA03	-0.11+0.36	-0.69+1.61	-1.71+0.68	0.41+3.05	1.41
	KACA	-0.11+0.52	-1.36+0.73	0.44+2.34	2.06+3.24	0.60
	SJJG	-0.35+0.17	1.39+0.84	0.56+0.75	-2.26+3.71	0.57
	SPG2	-0.02+0.22	0.21+0.36	-2.56+0.52	-4.66+0.81	0.48
	TBOH	0.03+0.28	-0.21+0.78	-1.89+0.39	1.30+1.06	0.91
Cont.	BSAT	-8.11+0.14	-4.34+0.11	-9.66+0.32	-16.02+0.25	2.33
	BTET	-2.07+0.07	-0.25+0.02	13.91+0.14	1.22+0.03	0.76
	LAIS	-3.53+0.03	-1.61+0.04	-8.05+0.07	-16.86+0.09	0.66
	LNNG	-5.30+0.06	-1.13+0.06	-8.50+0.14	-16.85+0.13	1.09
	MKMK	-5.02+0.06	-1.85+0.02	-10.19+0.12	-19.21+0.05	0.71
	MLKN	-1.95+0.05	0.94+0.03	6.72+0.11	-3.68+0.07	0.72
	MNNA	-0.90+0.03	0.72+0.03	3.68+0.07	-7.07+0.07	0.55
	MSAI	-0.57+0.05	0.68+0.06	7.37+0.13	-2.20+0.17	1.08
	NGNG	-8.29+0.11	-4.76+0.07	16.16+0.39	3.07+0.25	1.47
	PBJO	-1.42+0.05	-0.30+0.02	9.10+0.12	0.92+0.05	0.72
	PKRT	-1.61+0.03	3.43+0.03	2.25+0.12	-11.32+0.11	0.58
	PPNJ	-2.39+0.05	-3.28+0.03	-1.24+0.12	-6.11+0.07	0.76
	PRKB	-5.91+0.08	-3.74+0.04	-1.38+0.19	-15.38+0.09	1.10
	PSKI	-2.02+0.04	0.33+0.03	-0.50+0.11	-5.64+0.07	0.71
	SLBU	-3.75+0.31	-0.02+0.05	-31.52+0.74	-6.89+0.13	4.08
	TIKU	-2.02+0.04	-0.18+0.02	4.89+0.10	-0.60+0.05	0.66
				Average		0.86

Discussion

We used all available GPS data sets in Sumatra to estimate the postseismic decay and coseismic deformation of the 2007 Bengkulu earthquake, finding very small differences between the misfits of the logarithmic and exponential functions. Still, the logarithmic function has less misfit, a finding that coincides with previous analysis of postseismic decay after megathrust earthquakes, which have suggested that the logarithmic function better fits the GPS time series data compared to the exponential function (Ardika et al., 2015; Raharja et al., 2016).

As for coseismic displacement, we find that the GPS stations BTET and MSAI experienced insignificant displacements directed northwest (shown by red arrows in Figure 3). This displacement direction is opposite to the significant coseismic displacements observed by stations near the earthquake epicenter (shown in black in Figure 3). Unlike the displacements estimated at BTET and MSAI,

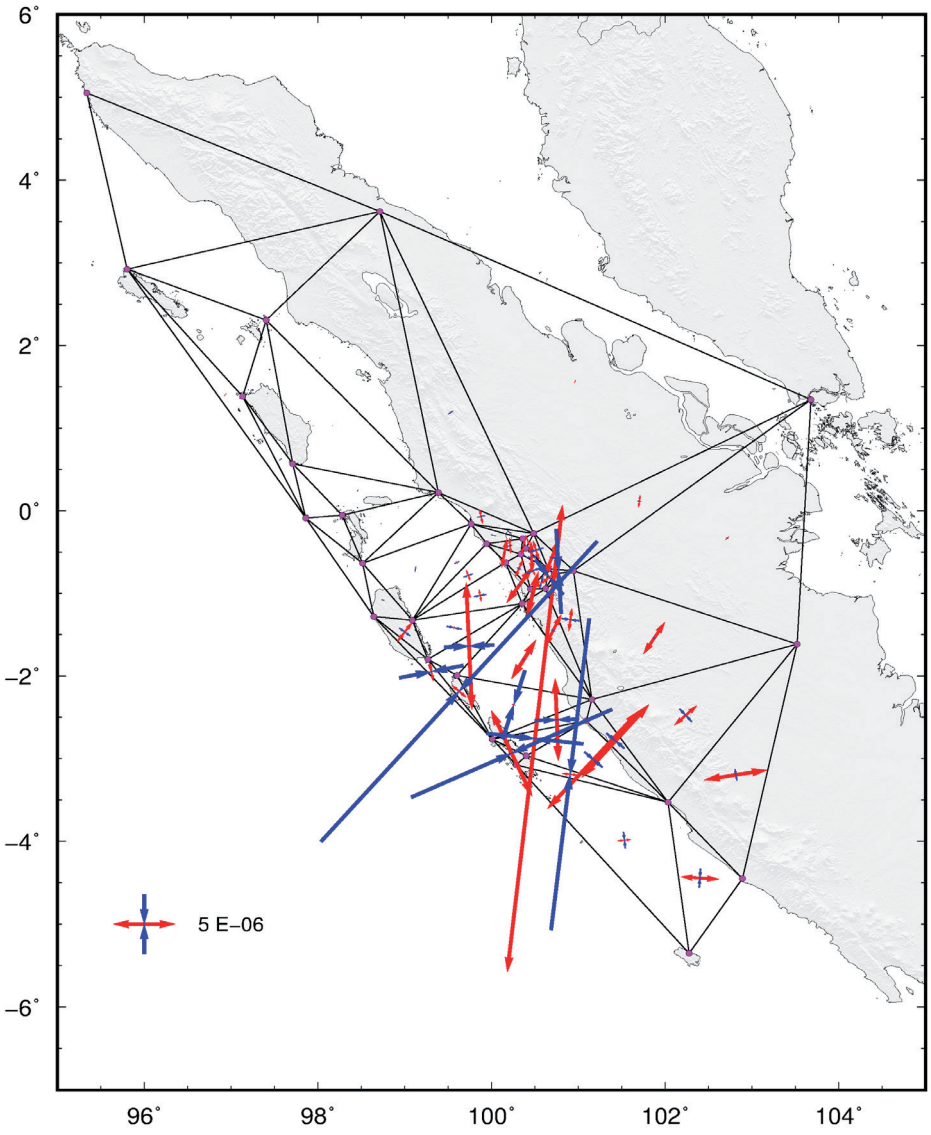

Figure 4. Coseismic principal strain is computed from triangular elements (boundaries indicated by solid lines) with nodes located at GPS stations (dots magenta). Red arrows suggest extension, while blue arrows indicate compression. Topography is from Becker et al. (2009).

these significant deformations are directed towards the coseismic rupture of the 2007 Bengkulu earthquake.

To investigate whether the GPS stations located in the northern part of the earthquake rupture were affected by the 2007 Bengkulu earthquake or by other deformations due to earthquake occurrences along the subduction zones, such as the 2004 Sumatra-Andaman earthquake (Gunawan et al., 2014) or the 2005 Nias earthquake (Hsu et al., 2006), we performed strain analysis based on the coseismic displacement data.

Results show significant extension directed towards the epicenter for GPS stations located in the south and east of BTET and MSAI stations, with the maximum estimated extensional strain of ~40 ppm. On the other hand, only very small extensional principal strain on the order of ~0.01 ppm was calculated along the subduction zone in the north of the BTET and MSAI stations (Figure 4).

Feng et al. (2015) suggested that the coseismic displacements of the 2007 Bengkulu earthquake were significant at MSAI and BTET stations. Our findings regarding the northwestward coseismic direction are similar to their analysis. However, our strain analysis suggests that the 2007 Bengkulu earthquake had minor effects at these sites. Finally, we showed that strain analysis could be very useful when analyzing ongoing deformation in a tectonically active region.

CONCLUSIONS

All available GPS data from continuous and campaign stations in Sumatra were used to analyze the coseismic displacement and postseismic decay and to estimate the strain of the 2007 Bengkulu earthquake. We find postseismic decay, estimated using a logarithmic function, of 46 days. Meanwhile, the maximum coseismic displacement was estimated at ~1.8m for GPS stations located north of the epicenter. Moreover, our principal strain estimation in the region suggests the maximum coseismic extensional strain of ~40 ppm.

ACKNOWLEDGEMENT

We thank two anonymous reviewers and the Editor for their thoughtful and thorough reviews. This research was partially funded by Ministry of Education, Research, Technology, and Higher Education of Indonesia No. LPPM.PN-1-06-2021.

REFERENCES

Alif, S.M., Meilano, I., Gunawan, E., Efendi, J., 2016. Evidence of postseismic deformation signal of the 2007 M8. 5 Bengkulu earthquake and the 2012 M8. 6 Indian Ocean Earthquake in Southern Sumatra, Indonesia, based on GPS data, Journal of Applied Geodesy, 10(2), 103–108.

Altamimi, Z., Collilieux, X., Métivier, L., 2011. ITRF2008: an improved solution of the international terrestrial reference frame, Journal of Geodesy, 85(8), 457–473.

Anugrah, B., Meilano, I., Gunawan, E., Efendi, J., 2015. Estimation of postseismic deformation parameters from continuous GPS data in Northern Sumatra after the 2004 Sumatra-Andaman earthquake, Earthquake Science, 28(5-6), 347–352.

Ardika, M., Meilano, I., Gunawan, E., 2015, Postseismic deformation parameters of the 2010 M7.8 Mentawai, Indonesia, earthquake inferred from continuous GPS observations, Asian Journal of Earth Sciences, 8, 127–133.

Becker, J.J., Sandwell, D.T., Smith, W.H.F., Braud, J., Binder, B., Depner, J., Fabre, D., Factor, J., Ingalls, S., Kim, S.H., Ladner, R., 2009. Global bathymetry and elevation data at 30 arc seconds resolution: SRTM30_PLUS, Marine Geodesy, 32(4), pp.355–371.

Feng, L., Hill, E.M., Banerjee, P., Hermawan, I., Tsang, L.L., Natawidjaja, D.H., Suwargadi, B.W., Sieh, K., 2015. A unified GPS-based earthquake catalog for the Sumatran plate boundary between 2002 and 2013, Journal of Geophysical Research: Solid Earth, 120(5), 3566–3598.

Gunawan, E., Sagiya, T., Ito, T., Kimata, F., Tabei, T., Ohta, Y., Meilano, I., Abidin, H.Z., Agustan, Nurdin, I., Sugiyanto, D., 2014. A comprehensive model of postseismic deformation of the 2004 Sumatra-Andaman earthquake deduced from GPS observations in northern Sumatra, Journal of Asian Earth Sciences, 88, 218–229.

Gunawan, E., Meilano, I., Abidin, H.Z., Hanifa, N.R., Susilo, 2016a. Investigation of the best coseismic fault model of the 2006 Java tsunami earthquake based on mechanisms of postseismic deformation, Journal of Asian Earth Sciences, 117, 64–72.

Gunawan, E., Maulida, P., Meilano, I., Irsyam, M., Efendi, J., 2016b. Analysis of coseismic fault slip models of the 2012 Indian Ocean Earthquake: Importance of GPS data for crustal deformation studies, Acta Geophysica, 64(6), 2136–2150.

Gunawan, E., Kholil M, Meilano I (2016c) Splay-fault rupture during the 2014 Mw7.1 Molucca Sea, Indonesia, earthquake determined from GPS measurements. Physics of the Earth and Planetary Interiors, 259, 29-33, DOI: 10.1016/j.pepi.2016.08.009.

Gunawan, E., Ghozalba, F., Syauqi, Widiastomo, Y., Meilano, I., Hanifa, N.R., Daryono, Hidayati, S., 2017a. Field Investigation of the November to December 2015 earthquake swarm in West Halmahera, Indonesia, Geotechnical and Geological Engineering, 35(1), 425–432.

Gunawan, E., Meilano, I., Hanifa, N.R., Widiyantoro, S.,2017b. Effect of coseismic and postseismic deformation on homogeneous and layered half-space and spherical analysis: Model simulation of the 2006 Java, Indonesia, tsunami earthquake, Journal of Applied Geodesy, doi: 10.1515/jag-2017-0009.

Gusman, A.R., Tanioka, Y., Kobayashi, T., Latief, H., Pandoe, W., 2010. Slip distribution of the 2007 Bengkulu earthquake inferred from tsunami waveforms and InSAR data, Journal of Geophysical Research: Solid Earth, 115(B12).

Gusman, A.R., Murotani, S., Satake, K., Heidarzadeh, M., Gunawan, E., Watada, S., Schurr,B., 2015. Fault slip distribution of the 2014 Iquique, Chile, earthquake estimated from ocean-wide tsunami waveforms and GPS data, Geophysical Research Letters, 42(4), 1053–1060.

Hanifa, N.R., Sagiya, T., Kimata, F., Efendi, J., Abidin, H.Z., Meilano, I., 2014. Interplate coupling model off the southwestern coast of Java, Indonesia, based on continuous GPS data in 2008–2010, Earth and Planetary Science Letters, 401, 159–171.

Herring, T.A., King, R.W., McClusky, S.C., 2010a. GAMIT Reference Manual Release 10.4. Report, pp 1–171, Massachussetts Institute Technology, Cambridge.

Herring, T.A., King, R.W., McClusky, S.C., 2010b, GLOBK Reference Manual: Global Kalman filter VLBI and GPS analysis program, Release 10.4. Report, 1–95, Massachussetts Institute Technology, Cambridge.

Herring, T., 2003. MATLAB Tools for viewing GPS velocities and time series, GPS solutions, 7(3), 194–199.

Hirose, H., Obara, K., 2006. Short-term slow slip and correlated tremor episodes in the Tokai region, central Japan, Geophysical Research Letters, 33(17).

Hsu, Y.J., Simons, M., Avouac, J.P., Galetzka, J., Sieh, K., Chlieh, M., Natawidjaja, D., Prawirodirdjo, L., Bock, Y., 2006. Frictional afterslip following the 2005 Nias-Simeulue earthquake, Sumatra, Science, 312(5782), 1921–1926.

Ito, T., Gunawan, E., Kimata, F., Tabei, T., Simons, M., Meilano, I., Agustan, Ohta, Y., Nurdin, I., Sugiyanto, D., 2012. Isolating along-strike variations in the depth extent of shallow creep and fault locking on the northern Great Sumatran Fault, Journal of Geophysical Research: Solid Earth (1978–2012), 117(B6).

Ito, T., Gunawan, E., Kimata, F., Tabei, T., Meilano, I., Agustan, Ohta, Y., Ismail, N., Nurdin, I., Sugiyanto, D.,2016. Co-seismic offsets due to two earthquakes (Mw 6.1) along the Sumatran fault system derived from GNSS measurements, Earth, Planets and Space, 68(1), 1, doi: 10.1186/s40623-016-0427-z.

Konca, A.O., Avouac, J.P., Sladen, A., Meltzner, A.J., Sieh, K., Fang, P., Li, Z., Galetzka, J., Genrich, J., Chlieh, M., Natawidjaja, D.H., 2008, Partial rupture of a locked patch of the Sumatra megathrust during the 2007 earthquake sequence, Nature, 456(7222), 631–635.

Konca, A.O., Hjorleifsdottir, V., Song, T.R.A., Avouac, J.P., Helmberger, D.V., Ji, C., Sieh, K., Briggs, R., Meltzner, A., 2007. Rupture kinematics of the 2005 Mw 8.6 Nias–Simeulue earthquake from the joint inversion of seismic and geodetic data, Bulletin of the Seismological Society of America, 97(1A), S307–S322.

Lorito, S., Romano, F., Piatanesi, A., Boschi, E., 2008. Source process of the September 12, 2007, Mw 8.4 southern Sumatra earthquake from tsunami tide gauge record inversion, Geophysical Research Letters, 35(2).

Marone, C.J., Scholtz, C.H., Bilham, R., 1991. On the mechanics of earthquake afterslip, Journal of Geophysical Research: Solid Earth (1978–2012), 96(B5), 8441–8452.

Murase, M., Kimata, F., Yamanaka, Y., Horikawa, S., Matsuhiro, K., Matsushima, T., Mori, H., Ohkura, T., Yoshikawa, S., Miyajima, R., Inoue, H., 2016. Preparatory process preceding the 2014 eruption of Mount Ontake volcano, Japan: insights from precise leveling measurements, Earth, Planets and Space, 68(1), 1.

Ohkura, T., Tabei, T., Kimata, F., Bacolcol, T.C., Nakamura, Y., Luis, A.C., Pelicano, A., Jorgio, R., Tabique, M., Abrahan, M., Jorgio, E., Gunawan, E., 2015. Plate convergence and block motions in Mindanao Island, Philippine as derived from campaign GPS observations, Journal of Disaster Research, 10(1), 59–66.

Okada, Y., 1992. Internal deformation due to shear and tensile faults in a half-space, Bulletin of the Seismological Society of America, 82(2), pp.1018–1040.

Pratama, C., Ito, T., Sasajima, R., Tabei, T., Kimata, F., Gunawan, E., Ohta, Y., Yamashina, T., Ismail, N., Nurdin, I., Sugiyanto, D., Muksin, U., Meilano, I., 2017. Transient rheology of the oceanic asthenosphere following the 2012 Indian Ocean Earthquake inferred from geodetic data, Journal of Asian Earth Sciences, 147, 50–59.

Raharja, R., Gunawan, E., Meilano, I., Abidin, H.Z., Efendi, J., 2016. Long aseismic slip duration of the 2006 Java tsunami earthquake based on GPS data, Earthquake Science, 29(5), 291–298.

Rhie, J., Dreger, D., Bürgmann, R., Romanowicz, B., 2007. Slip of the 2004 Sumatra–Andaman earthquake from joint inversion of long-period global seismic waveforms and GPS static offsets, Bulletin of the Seismological Society of America, 97(1A), S115–S127.

Savage, J.C., Prescott, W.H., 1978, Asthenosphere readjustment and the earthquake cycle, Journal of Geophysical Research: Solid Earth, 83(B7), 3369–3376.

Tung, S,. Masterlark, T., 2016. Coseismic slip distribution of the 2015 Mw7. 8 Gorkha, Nepal, earthquake from joint inversion of GPS and InSAR data for slip within a 3-D heterogeneous Domain, Journal of Geophysical Research: Solid Earth, 121, 3479–3503.

Wallace, L.M., Webb, S.C., Ito, Y., Mochizuki, K., Hino, R., Henrys, S., Schwartz, S.Y., Sheehan, A.F., 2016. Slow slip near the trench at the Hikurangi subduction zone, New Zealand, Science, 352(6286), 701–704.

Wessel, P., Smith, W.H.F., 1998. New, improved version of Generic Mapping Tools released, Eos Trans. AGU, 79, 579.